論文 / 著書情報
Article / Book Information

Title(English)	Empirical correlations for thermal-hydraulic characteristics of compact heat exchangers with microchannels
Authors(English)	Motoaki Utamura, Yasuyoshi Kato, Konstantin Nikitin, Ngo T., L., Takao Ishizuka
Citation(English)	5th Korea-Japan Symposium on Nuclear Thermal-Hydraulics and Safety, NTHAS5-N001, pp. 733-740
発行日 / Pub. date	2006, 11

NTHAS5: Fifth Korea-Japan Symposium on Nuclear Thermal Hydraulics and Safety
Jeju, Korea, November 26- 29, 2006

NTHAS5-N001

EMPIRICAL CORRELATIONS FOR THERMAL-HYDRAULIC CHARACTERISTICS OF COMPACT HEAT EXCHANGERS WITH MICROCHANNELS

Motoaki Utamura[1*], Yasuyoshi Kato[1], Konstantin Nikitin[1] , Tri Lam Ngo[1] and Takao Ishizuka[1]

[1] *Research Laboratory for Nuclear Reactors*

Tokyo Institute of Technology,

2-12-1 O-okayama, Meguro-ku, Tokyo, 152-8550 Japan

tel:+81357343293

fax:+81357342959

E mail: utamura@rccre.titech.ac.jp

ABSTRACT

Incorporating "integral method" proposed here, a set of empirical correlations of local heat transfer coefficient and pressure loss coefficient are newly derived based on experiments using microchannel heat exchanger (MCHE) with supercritical carbon dioxide as heating medium and water as coolant. They are $\boldsymbol{Nu= C_1Re^{0.8}Pr^{0.6}}$, $\boldsymbol{C_1=0.0473}$, $\boldsymbol{f= C_2Re^{-0.25}}$, $\boldsymbol{C_2=2.294}$.The same correlation of Nusselt number is found applicable to both fluids and its value is almost two times larger than Dittus Boelter correlation. It was also shown that the above form is applicable to a wide range of geometry with the values of constants C_1 and C_2 changed. For example, the correlations with $\boldsymbol{C_1=0.0102}$ and $\boldsymbol{C_2=0.156}$ are applicable to an existing tubular heat exchanger. Accuracy of both correlations is confirmed within 5% errors for MCHE with S-shaped fins in the range of pressures 9~12.5MPa and temperatures 280~390K. Based on the correlations, design method of heat exchanger is also developed.

1. INTRODUCTION

Compactness and efficiency improvement of heat exchangers are important, particularly for cost reduction, in all energy system: modern air-conditioning, heat pumps, refrigeration, and waste heat recovery systems for variety of residential, industrial, automotive and process industry applications. A Printed Circuit Heat Exchanger (PCHE) is a promising candidate for compact heat exchangers. Two technologies are applied to manufacture the PCHE: photo-etching and diffusion bonding.

Compactness of the heat exchangers is usually expressed by using the Colburn *j* factor, given as

$$j = \frac{D_h}{4L} \mathrm{Pr}^{2/3} N , \tag{1}$$

where $N=NTU$ (Number of Thermal Units), and

$$N = (T_{out} - T_{in}) / \Delta T_{LMTD} . \tag{2}$$

Reduction of the hydraulic diameter engenders a decreased active length L or heat exchanger size at the same Colburn j factor, Pr and N conditions, as shown in Eqs. (1) and (2) (Hesselgreaves, 2001). The hydraulic diameter is easily reducible in PCHEs because photo-etching technology can mill small flow channels. Such reductions are not achieved easily in usual plate fin exchangers because costs of plate fin bonding increase with increase of fin density or reduced hydraulic diameter. For PCHE, hydraulic diameter reduction is not limited by the manufacturing cost increment because of utilization of chemical etching process for forming channel configuration. PCHE, however, has a pressure drop larger than a tubular heat exchanger. To overcome this drawback, a previous study introduced a new PCHE with the S-shaped fins, what we call microchannel heat exchanger (MCHE). MCHE reduces the pressure drop by four times less than that of PCHE while retaining high heat-transfer performance (Nikitin *et al.*,2004;Tsuzuki *et al.*,2005), thereby extending the PCHE application field to lower-pressure plants.

Moreover, the diffusion bonding technology utilized in MCHE maintains the parent material strength because of no flux, braze or filler exist in the heat exchanger core. This provides high capability of corrosion and temperature resistance.

The purpose of this study is to expand applicability of the new MCHE from the gas (CO_2)-gas (CO_2) heat exchanger of the recuperator for the CO_2 gas turbine cycle system (Kato *et al.*, 2004) to a gas (CO_2)-liquid (H_2O) heat exchanger or a hot water supplier for a residential use.

2. METHOD OF EXPERIMENT

Taking a commercial hot water supplier as an example, mock up experiments were carried out using a microchannel heat exchanger. It is made of plates forming flow channel with brand-new S shaped fins(S-fin).

2.1 Experimental Facility

An experimental facility was built to measure thermal-hydraulic parameters of supercritical CO_2 on the MCHE hot water supplier inlet and outlet under different operating conditions (see Fig. 1). The new MCHE hot water supplier was designed and manufactured with a heat load of 4.6 kW. To limit heat loss from the surfaces of MCHE test section during the experiments, it was insulated by 5 cm thickness of ceramic wool, 10 cm thickness of rock wool and 10 cm of glass wool layers to ensure the heat loss could be neglected in the experimental data reduction process. In order to avoid the influence of heat conduction to and from adjacent piping, temperatures of both fluids, CO_2 and water at both inlets and exits of the test section were measured at the plenums of the heat exchanger.

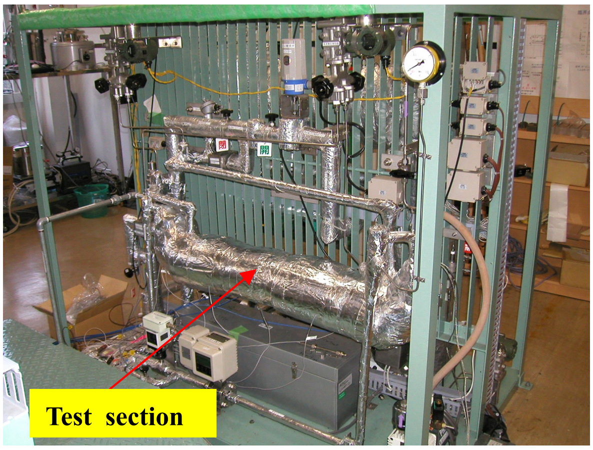

Fig.1 Experimental facility

2.2 Operation of Experimental Facility

A schematic diagram of the experimental loop is shown in Fig. 2. Carbon dioxide from the low pressure tank is compressed by the oil compressor. High-pressure gas is heated by an electric heater 1 (1.9 kW) after passing through gas cooler 1 and the oil separators. The resulting CO_2 is forwarded through a turbine type flow meter to the inlet of the MCHE-HWS which is being tested. The pressure of CO_2 gas discharged from the MCHE outlet is reduced by a flow rate control expansion vale and transferred to an electric heater 2 (2.2 kW). CO_2 gas is heated by an electric heater 2 (2.2 kW) in order to maintain the CO_2 in gas phase. Because of adiabatic expansion process, the pressure of CO_2 is downed to low pressure, so the temperature becomes saturated temperature. After heating by heater 2, CO_2 gas temperature is adjusted by the gas cooler 2 to obtain a suitable CO_2 gas temperature before returned to the CO_2 low pressure tank. The flow meter of the CO_2 side is installed just after gas cooler 2. The city water is directly supplied to the H_2O side inlet; the city water temperature can be adjusted using the chiller/warmer to meet the required testing conditions.

Experimental procedure is as follows. While water inlet pressure in not controlled (~0.2-0.3MPa), CO_2 inlet pressure is controlled by compressor and bypass valve. CO_2 inlet temperature is controlled by Heater 1 and Cooler 1 while water inlet temperature by additional heater/cooler (not shown). Water outlet temperature is controlled by water flow rate control system (not shown). CO_2 flow rate is controlled by CO_2 flow rate control system (not shown). Only CO_2 flow rate is varied during experiment. Water flow rate is obtained as a result of water outlet temperature control.

The experimental facility requires about 3 hours reaching a steady state condition from the beginning of an experimental run. When some parameters are changed (e.g. a flow rate) it requires 30 minutes to approach a new steady state condition. A steady state condition was determined as a condition when the fluctuation of measured parameters is well within the range of measurement accuracy for at least 10 minutes. The CO_2 and H_2O temperatures, pressures and pressure drops were directly measured and used in the further calculations while the flow rate value was corrected according to the measured CO_2 temperature and pressure near the location of the flow meter. The corrective dependencies were provided by the manufacturer of the experimental loop. All the values were then averaged over 5 minute interval. Throughout day of the experiment the inlet pressure and temperature of hot/cold side were kept constant while the set value of the flow rate was changed in 5 kg/h increments.

2.3 Instrumentation

The CO_2 inlet pressure of the MCHE was measured using a pressure gauge transducer with an accuracy of ±0.25% over the full range of 13 MPa. The pressure drop was measured using a differential pressure gauge with an accuracy of ±0.15% over the full range of 400 kPa for the CO_2 side and 50 kPa for H_2O side. The T-type (Copper/Constantan) thermocouples with accuracy of ±0.5°C at the range of 40–125°C were used for temperature measurement in both cold and hot side. Thermocouples were inserted into the inlet and outlet of MCHE's distributors. All thermocouples were calibrated at a water boiling and ice point. The CO_2 flow meter accuracy was ±5% over the full range of 20–88 kg/h.

All parameters, including inlet/outlet CO_2 and H_2O temperatures and pressures, flow rates, and pressure drops for both sides, were recorded automatically with a 0.5-Hz sampling frequency.

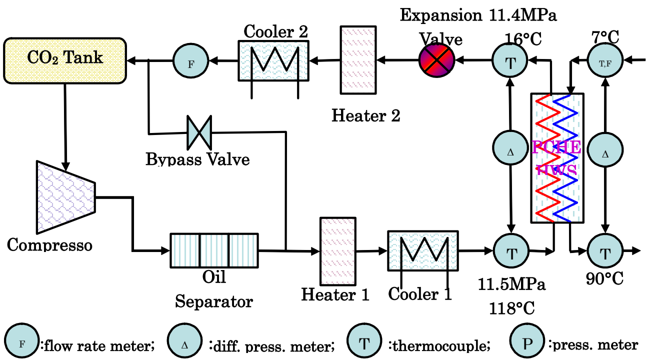

Fig. 2. Flow diagram of supercritical CO_2 experimental loop

2.4 Heat Exchanger Test Pieces

2.4.1 Macroscopic Configuration of New MCHE

The new MCHE is a high-integrity plate type heat exchanger. The MCHE is constructed from flat copper plates that have fluid flow passages chemically milled into them. This technique is similar to that used in the manufacture of electronic printed circuit boards. The plates are then diffusion bonded together into blocks to form a heat exchanger core of the required capacity. The new MCHE has core dimensions of 870×78×14mm as shown Fig.3. This MCHE includes two CO_2 and one H_2O plates combined in sandwich structure, so-called double banking. Hot side and cold side fluid are CO_2 and water respectively. Flow direction of fluids is countercurrent in order to enhance heat transfer.

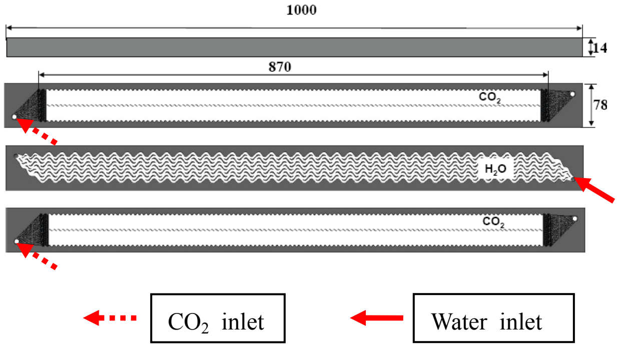

Fig.3 Configuration of microchannel heat exchanger

Fig.4 shows transparent plan view of the central part of the heat exchanger together with vertical cross section view. The total number of flow channels is 54 and 4 for the hot and cold sides, respectively. The flow channel is formed in sine wave by S-shaped fins.

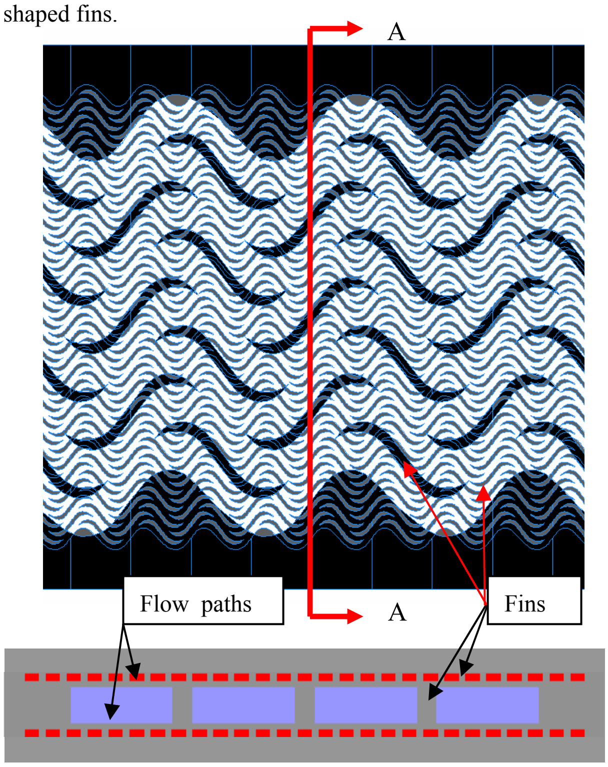

A-A Cross-section

Fig. 4 Hot and cold plate configuration

small = CO_2 side fins and large = H_2O side fins

2.4.2 S-shaped Fin Thermal-Hydraulic Parameters

CFD analyses were carried out to find S-fin configuration to give characteristics of enhanced heat transfer with pressure drop as small as possible. Results are shown in Table 1 with reference to Fig.5 that depicts fin geometrical parameters.

To derive thermo-hydraulic parameters A, A_c and D_h shown above, following assumptions and definitions were adopted.

1) Heat transfer area A is defined as the sum of surface area where fluid is attached. Therefore, side wall area of fins is included. This is appropriate because heat resistance of channel wall made of copper is negligibly small, being one hundred times less than that due to heat transfer.
2) Free flow area of heat exchanger A_c is defined as the free volume V divided by the length of the heat exchanger L.
3) As the flow path is formed by network and geometry is varied in the direction of apparent principal flow, then hydraulic diameter D_h is defined here by

$$D_h = \frac{4V}{A}. \tag{3}$$

Eq.(3) coincides with usual definition of D_h in the case that geometry is unchanged along flow path. In the case of MCHE, using the relation $V=A_cL$ by assumption 2), Eq.(3) reduces to the usual form of $4A_c/a$ where a is average wetted perimeter defined by $a=A/L$.

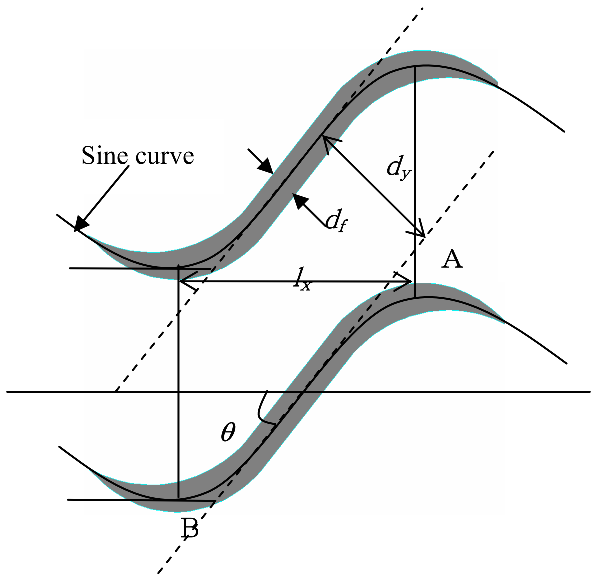

Fig.5 Geometrical parameters to define S-fin

Table 1 Summary of S-fin Design Parameters

Items	CO_2 side	Water side
Fin angle θ, (°)	52	52
Fin length |AB|, (mm)	4.8	14.4
Fin width d_f, (mm)	0.4	1.2
Channel depth, (mm)	0.47	2.5
Channel width d_y- d_f, (mm)	0.87	6.17
Hydr. dia. D_h, (mm)	0.59	3.40
No. of Channels N_{ch} (-)	54	4
Heat trans. area, A (m^2)	0.225	0.109
Free flow area, A_c (m^2)	27.1×10^{-6}	96.5×10^{-6}

2.4.3 ECO_CUTE Heat Exchanger

Existing hot water supplier (ECO_CUTE trademark in Japan) was also tested for comparison. The ECO_CUTE heat exchanger is among the tube heat exchanger type, in which three channels of super critical CO_2 cover a channel of city water. The cross-section view and heat exchanger's structure are shown in Fig. 6. The ECO_CUTE heat exchanger's overall dimension is 154×428×193 mm formed by tube's length of 14 m. The detailed specification parameters are given in Table 2.

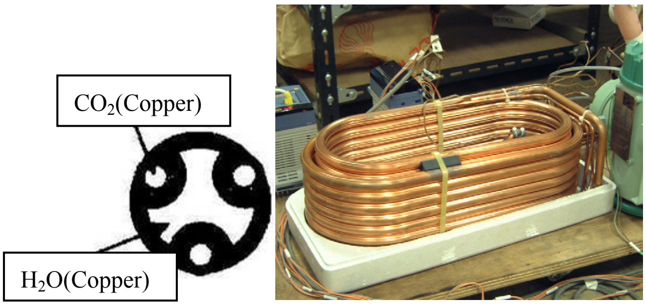

a) Cross-section b) ECO CUTE heat exchanger

Fig.6 Eco-cute heat exchanger test section

Table 2 Dimension of ECO_CUTE

Items	CO_2 side	H_2O side
Dimension (mm)	154×428×193	
Equivalent length L(m)	14	14
Hydraulic diameter D_h(mm)	2.5	7.0
Wall thickness (mm)	0.5	1.0
Free flow area A_c (m^2)	14.7×10^{-6}	38.5×10^{-6}
Heat transfer area A(m^2)	0.336	0.308

2.5 Experimental Conditions

The inlet temperature of CO_2 side is set at about 100° C and 118° C while the pressure reach up to 11.0 to 12.5 MPa. This hot super critical CO_2 heat up the city water from 7° C or 25° C to 85° C, 90° C or 95° C throughout the new MCHE or double tube heat exchanger. The city water's pressure is estimated circa 0.25 MPa. The flow rate of super critical CO_2 is changed from about 25 kg/h to about 80 kg/h for each case of setting pressure or temperature. The outlet temperature of CO_2 side or the flow rate of H_2O is the dependent parameter resulting from heat exchange in test sections. More than fifty test cases were run. Those experimental conditions are clearly given in Table 3. It should be noted that both Reynolds number and Prandtl number varies not only among test runs but also within the heat exchanger. It is because the state of super critical CO_2 passes by the vicinity of critical state point 7.38MPa,304K(31degC) where isobaric specific heat of CO_2 varies so much within the heat exchanger as shown in Fig.7.

Table 3 Experimental Conditions for MCHE

		CO_2 side		Water side	
		min	max	min	max
Press. (MPa)		9.5	12.6	~0.25	
Flow rate(kg/h)		26.8	81.1	17.4	50.4
Temp.(deg C)	inlet	99.2	120.4	4.3	27.6
	outlet	19.4	45.6	84.9	93.4
Heat load(W)		1604	4628	1604	4628
Reynolds No.	Inlet	7351	19773	110	587
	Outlet	1832	9960	510	1627
Prandtl No.	Inlet	1.03	1.05	5.74	11.43
	Outlet	2.06	2.89	1.89	2.10

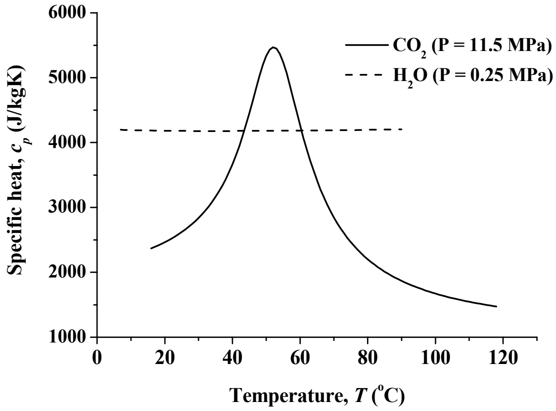

Fig.7 Variation of specific heat CO_2 in ECO-CUTE operation

3. METHOD OF ANALYSIS

3.1 Integral Method

The heat exchange performance of the test sections is estimated in terms of an average overall heat transfer coefficient. However, it is found that nonlinear characteristic is occurred for these range of operating conditions as illustrated in Fig. 8 in which ΔT denotes difference in temperatures of hot and cold fluids. Therefore, the famous Logarithmic Mean Temperature Difference Method (LMTD) is no longer applicable for these cases.

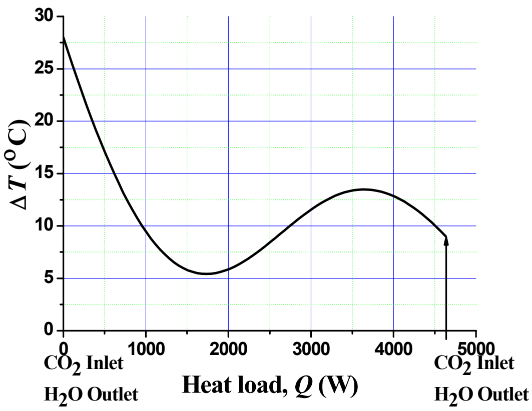

Fig. 8 Temperature difference ΔT between fluids in hot and cold sides as function of heat load

Thus, the LMTD equation is modified to an integral form, what we call integral method, to evaluate the average overall heat transfer coefficient. The methodology is described in the following. Heat exchange rate dQ in an infinitesimal region dA of an heat exchanger can be expressed by $dQ=U\Delta TdA$. Its integration yields to a fundamental integral equation:

$$\int_0^{Q_0} \frac{dQ}{\Delta T} = \int_0^{A_0} UdA \,. \qquad (4)$$

We define average overall heat transfer coefficient $\overline{U}$ and average temperature difference $\Delta\overline{T}$ as

$$\overline{U} \equiv \frac{1}{A_0}\int_0^{A_0} UdA \,, \qquad (5)$$

$$\Delta\overline{T} \equiv Q_0 \Big/ \int_0^{Q_0} \frac{dQ}{\Delta T(Q)} \qquad (6)$$

$$\Delta T(Q) = T_{hot}(Q) - T_{cold}(Q)$$

$$Q_0 = W_{cold}(h_{cold,out} - h_{cold,in}) \,. \qquad (7)$$

Received heat load (Eq.(7) was used for analysis because experiment was aimed at development of hot water supplier as well as higher accuracy of measurement of the flow rate in water side was observed.

Right hand side of Eq.(6) can be executed using $\Delta T(Q)$ as shown in Fig.8 which can be derived from measurements of Q_0, inlet temperature conditions and flow conditions. Then, from measurements by use of Eq.(5) and (6), average overall heat transfer coefficient $\overline{U}^{exp.}$ averaged over the entire heat exchanger is written by

$$\overline{U}^{exp.} = \frac{Q_0}{A_0 \Delta\overline{T}} \,. \qquad (8)$$

In the above, CO_2 and water thermo physical properties are taken by PROPATH package (Ito *et al.,*1990). Physical properties were evaluated with pressure effect taken into consideration. It is assumed that the pressure changes linearly along the length of heat exchanger.

3.2 Correlation for Nusselt Number

Two assumptions were made;

1) The same equation can be applied to both fluids. It is because the geometry of the central part of flow channel is similar between both fluids.
2) It is possible to express the Nusselt number as the product of polynomials of Reynolds and Prandtl number as

$$Nu = C_1 \times Re^m Pr^n \qquad (9)$$

where Reynolds number was evaluated by average velocity.
Otherwise, local heat transmission coefficient U_{coldt} based on cold side heat transfer area is generally written by

$$U_{cold}A_{cold} = 1 \Big/ \left(\frac{1}{\alpha_{hot}A_{hot}} + \frac{\Delta t_{wall}}{\lambda A_{wall}} + \frac{1}{\alpha_{cold}A_{cold}}\right)$$

(10)

,where heat transfer coefficient α is related to Nu as $\alpha = \frac{\lambda Nu}{D_h}$ from the definition of Nusselt number.

However, the conductivity of copper is 387W/(mK) while the wall thickness is about o.5mm. Then the product of $\Delta T_{wall} / \lambda\, A_{wall}$ is one hundred times less than other terms and was neglected. Then, by substituting Eq.(11) into Eq.(12) and using the assumption 1), we have

$$U_{cold} = \frac{C_1 A_{hot}\lambda_{cold}\lambda_{hot}Re^m_{hot}Pr^n_{hot}Re^m_{cold}Pr^n_{cold}}{D^{hot}_h A_{cold}\lambda_{cold}Re^m_{cold}Pr^n_{cold} + D^{cold}_h A_{hot}\lambda_{hot}Re^m_{hot}Pr^n_{hot}} \equiv C_1 F$$

(11)

Note that C_1 is common to that of Eq.(9) and physical properties were evaluated by local bulk fluid temperature.
With the preparation mentioned above, using Eq.(5) and (11), the calculation of average overall heat transfer coefficient can be made through execution of integration by change in variables as

$$\overline{U}^{calc.} = \frac{1}{A_0}\int UdA = \frac{1}{A_0}\int U(Q)\frac{dA}{dQ}dQ \cong$$

$$\frac{1}{A_0}\int U(Q)\frac{\Delta\overline{T}}{\Delta T(Q)}dQ = \frac{C_1}{M}\sum_{i=1}^{M} F_i \frac{\Delta\overline{T}}{\Delta T_i} \equiv C_1\overline{F}$$

(12)

Provided power indices *m* and *n* are determined in prior, then $\overline{F}$ can be calculated and constant C_1 may be obtained by application of least square method i.e. $\sum_{i=1}^{P}(U_A^{exp.} - C_1 F_{ave})^2 \Rightarrow min.$ where P is the number of data. The number of sub-divisions M of the heat exchanger was typically one thousand.

With the aid of Eq.(9), profiles of Nusselt number on both sides of CO_2 and water could be separately obtained from measurement. Taking the ratio $R_{Nu}, R_\lambda, R_A, R_{D_h}$,

$$Nu^{cold} = \frac{U^{cold}D^{cold}_h}{\lambda_{cold}}\left(\frac{R_\lambda R_A R_{Nu}}{R_{D_h}} + 1\right),$$

$$Nu^{hot} = \frac{1}{R_{Nu}} Nu^{cold} \qquad (13)$$

$$\overline{Nu} = \sum_{i=1}^{M} Nu_i \Big/ M$$

3.3 Pressure Loss Coefficient

Once correlation for Nusselt number is obtained, then pressure loss could be calculated by the following integral

$$\Delta P = \int_0^L \varphi dl = \int_0^{Q_0} \varphi \frac{dl}{dQ} dQ = \int_0^{Q_0} \varphi \frac{LdQ}{UA_0\Delta T}$$

$$\varphi \equiv f\frac{G^2}{2\rho D_h} \qquad (14)$$

Here, functional form of $f = C_2 Re^{-r}$ is assumed for CO_2 side taking account of the range of Reynolds number as shown in Table 3. C_2 and r were best fitted against pressure drop measurements by means of least square method,

$$\sum_{i=1}^{p}(\Delta P^{\exp} - \Delta P^{calc.})^2 \Rightarrow m\,in.$$

4. RESULTS AND DISCUSSIONS

4.1 Thermal Performance

4.1.1 Empirical Correlation for Nusselt Number

Based on ECO-CUTE experimental results as shown in Fig. 9 and CFD analysis for MCHE in Fig.10, the power indices were determined. Literatures show power index of Reynolds number 0.8 is applicable to a variety of fluids except super critical CO_2. The present experiment using ECO-CUTE tubular heat exchanger verified the figure 0.8 is applicable to CO_2, too.
The power index of Prandtl number is varied from 0 to 0.8. It is found that at $Pr^{0.6}$ the best curve to fit FLUENT numerical simulation result (Fluent Inc., 2003; Ngo *et al.,*2005) for MCHE can be obtained as illustrated in Fig.10. Therefore, the Nusselt number finally could be obtained in following form:

$$Nu = C_1 \times Re^{0.8} Pr^{0.6} \qquad (15)$$

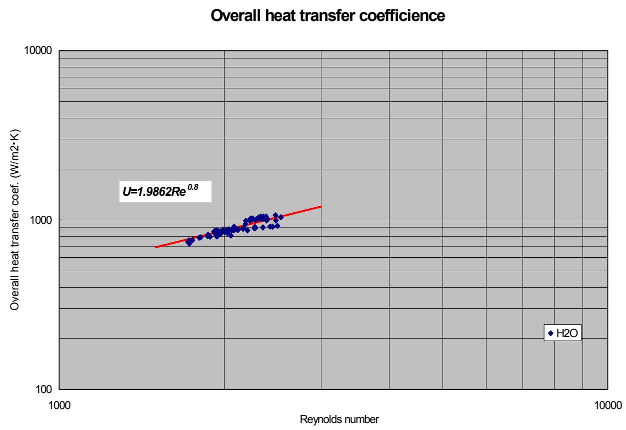

Fig.9 Influence of Reynolds number on average overall heat transfer coefficient

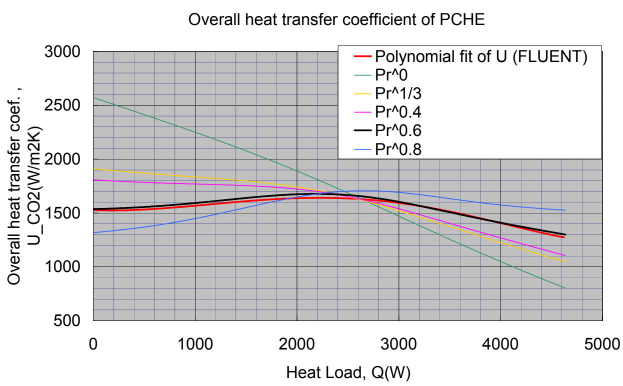

Fig.10 Profile of heat transmission coefficient inside MCHE

Fig. 11 shows the results. Both water and CO_2 data are in line and application of the same equation (Eq.(15)) was proved to be valid. Both data from MCHE and tubular were seen well correlated by the same functional form. Best fitted value of C_1 gives C_1=0.0473 for MCHE and C_1=0.0102 for tubular respectively. Fig. 12 shows that prediction error by the present correlation applied to MCHE was 5%. Moreover, FLUENT calculation result was best fitted with C_1=0.0454 being 4% less than that of the correlation. Also, very good agreement was obtained. From this about five times better thermal performance could be expected in S-fin MCHE rather than an existing ECO-CUTE tubular heat exchanger.

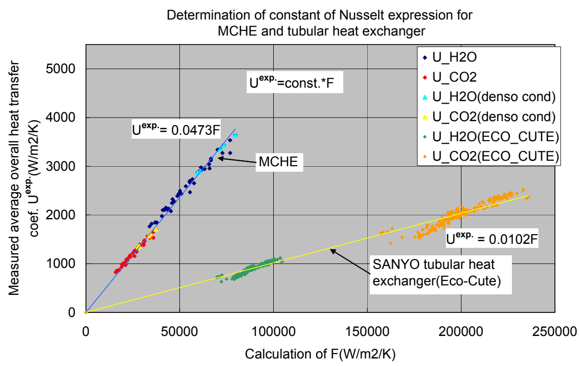

Fig. 11 Relation of $\overline{U}^{\exp.}$ and $\overline{F}$

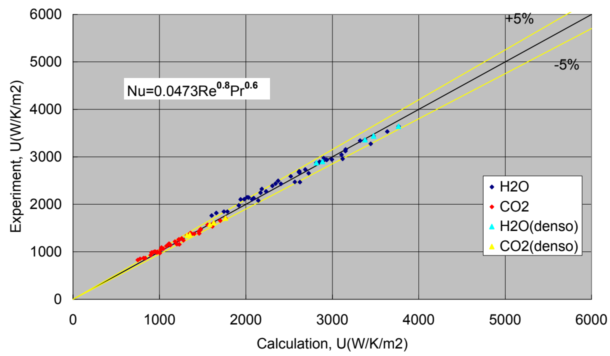

Fig. 12 Comparison of $\overline{U}^{\exp.}$ and $\overline{U}^{calc.}$

Fig.13 illustrates relation between measured Nusselt number and the value of Nu/C_1 (=$Re^{0.8}Pr^{0.6}$) calculated by Eq.(15) and averaged over an entire heat exchanger. Thermal performance of S-fin MCHE is two times larger than prediction by Dittus Boelter for turbulent flow in tube.

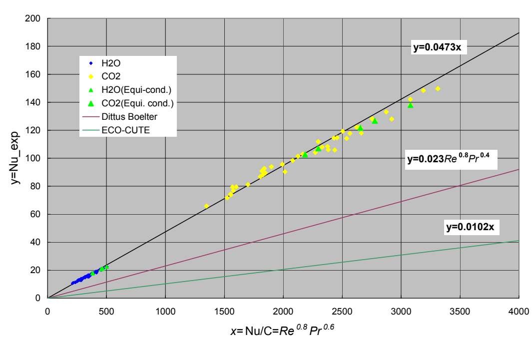

Fig. 13 Comparison of Nusselt number

Nusselt number for each fluid separated but present in the same line, which proves again the validity of the assumption 1) in section 3.2.

4.1.2 Profile of Thermal Performance Parameters

Fig. 14 shows temperature profile of both fluids. Cold means water and hot, CO_2. It compares prediction by Eq.(15) with measured data. Good agreement was obtained in the entire region of MCHE. Four data at right and left end exhibit fluid temperatures measured at inlet and exit plenums.

Fig.15 exhibits profiles of overall heat transfer coefficient and heat transfer coefficient of both fluids. Heat transfer is restricted virtually by water side heat transfer due to bigger hydraulic diameter. This comes from the practical requirement of avoiding deposits due to water crud.

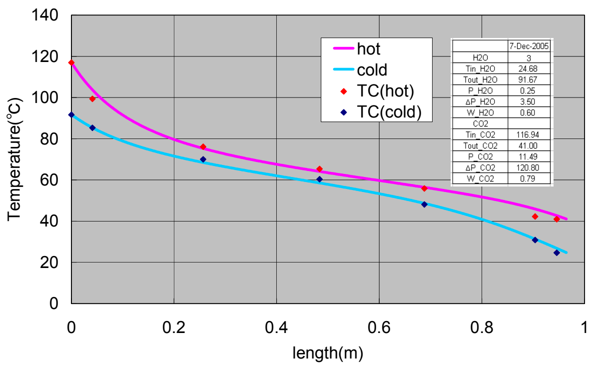

Fig. 14 Predicted and measured temperature profile in MCHE

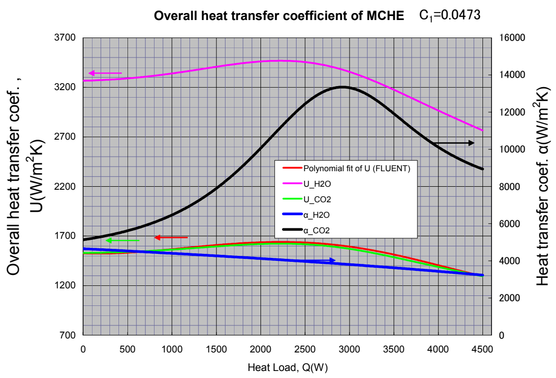

Fig.15 Calculated profile of OHTC and HTC in MCHE

4.2 Hydraulic Performance

4.2.1 Empirical Correlation for Pressure Loss Coefficient

From COP (coefficient of performance) point of view, pressure drop in CO_2 side is important. Parametric studies focusing on CO_2 side were conducted to obtain optimum value for power index r of Reynolds number $f = C_2 Re^{-r}$. Best fitted value was r=0.25 quite coincidently with the same as is observed in Blasius formula. Fig.16 shows results. Best fitted value of C_2 was C_2=2.294 for MCHE and C_2=0.155 for tubular respectively. Prediction error was within 5% for MCHE and 10% for tubular type heat exchange respectively. Generally, unlike PCHE, pressure drop of MCHE is found about four times less than that of tubular type under the condition of equivalent heat load. It comes from the fact that in tube, as we already noticed, Nusselt number is five times smaller at the same Reynolds number. Thus, in order to maintain equivalent heat load, mass flux have to be increaseed, which results in higher pressure drop. It is suggested that pressure loss coefficient as well as Nusselt number has a form common to different flow configurations. It is clarified that drawback inherent in conventional PCHE is removed by MCHE.

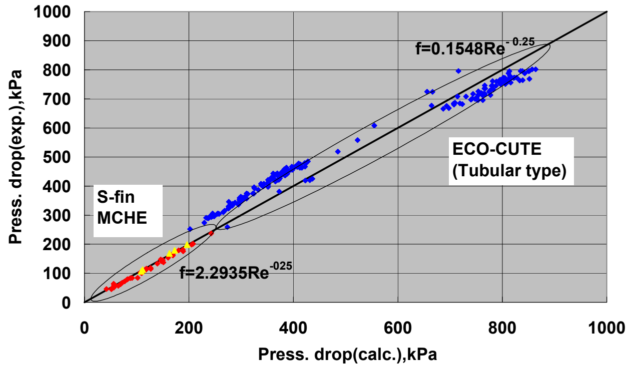

Fig.16 Comparison of calculation with experiment

4.3 Design Procedure of MCHE

Thermal hydraulic design process is discussed in this section where well known LMTD method is no longer applicable due to non-linear characteristics of physical properties. It is common that heat exchanger is designed under the condition that heat duty, inlet conditions (temperature and mass flow), one of two exit temperatures and maximum allowable pressure drop are given. In MCHE design, once S-fin geometry is given and thermal hydraulic correlations fixed with proper constants C_1 and C_2, it reduces to the choice of the number of flow channels and resultant length of the heat exchanger.

Fig.17 gives schematic flow of such design process.

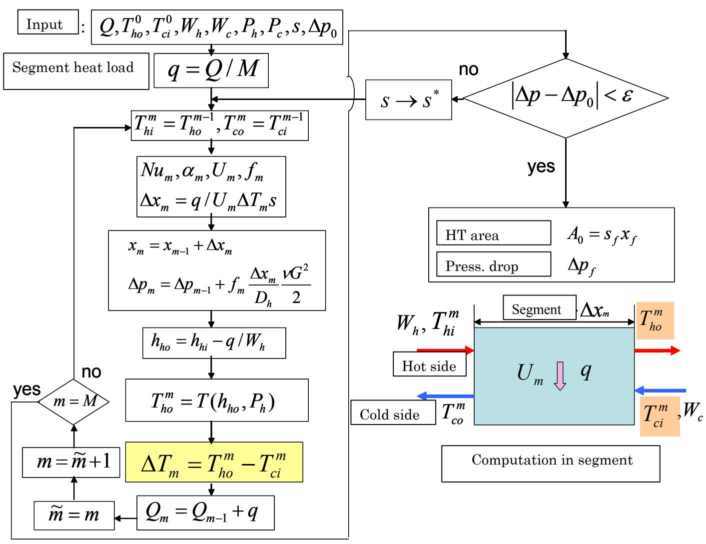

Fig.17 Thermal hydraulic design flow of MCHE

Following this procedure, reverse problem was solved, i.e. given experimental conditions and measurements length of the MCHE was calculated to every test run. Results were shown in Fig.18. Averaged calculation value overestimated the actual length by 1%. Data scattered around the mean value is +6%-8%. Considering experimental uncertainties involved, it is concluded the present correlations are accurate enough to design heat exchanger alike.

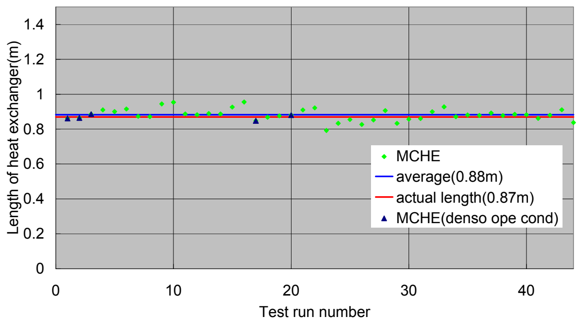

Fig.18 Calculated heat exchanger length vs. actual one

5. CONCLUSIONS

The thermal-hydraulic performance of new microchannel heat exchanger (MCHE) has been investigated, experimentally in the range of pressures 9~12.5MPa and temperatures 280~390K. Heating media were super critical carbon dioxide for hot side and water for cold side. The empirical correlations of Nusselt number and pressure loss coefficient were proposed to predict thermo-hydraulic characteristics for both MCHE and tubular heat exchanger for hot water supplier. It was found that the thermal-hydraulic performance of MCHE is about 4.7 times better than that of tubular heat exchanger while the pressure drops of both sides are kept lower.

Also, the CFD calculation by FLUENT has been experimentally validated. The deviation between FLUENT calculation and experimental results is about 5% for heat transfer performance.

ACKNOWLEDGEMENT

Work partly performed under the program of "Strategic development of Technology for Efficient Energy Utilization-Project of Fundamental Technology Development for Energy Conservation" sponsored by NEDO.

NOMENCLATURE

A	Heat transfer area	[m^2]
A_c	Free flow area ($\equiv V/L$)	[m^2]
D_h	Hydraulic diameter	[m]
F	Function (Eq.(11))	[W/m^{2}K]
f	Pressure loss coefficient	[-]
G	Mass flux($\equiv W/A_c$)	[kg/ m^{2}s]
h	Specific enthalpy	[W/kg]
L	Length of heat exchanger	[m]
LMTD	Log mean temperature difference	[K]
MCHE	Microchannel heat exchanger	
N	Number of flow channels	[m]
Nu	Nusselt number($\equiv \alpha D_h/\lambda$)	[-]
OHTC	Overall heat transfer coefficient	[W/m^{2}K]
P	Pressure	[Pa]
Pr	Prandtl number	[-]
Q	Heat load	[W]
R	Ratio defined by Eq.(13)	[-]
Re	Reynolds number($\equiv G D_h/\mu$)	[-]
T	Temperature	[K]
U	Overall heat transfer coefficient	[W/m^{2}K]
V	Free volume of heat exchanger	[m^3]
W	Mass flow of fluid	[kg/s]
	Greek	
α	Heat transfer coefficient	[W/m^{2}K]
λ	Heat conductivity	[W/mK]
μ	Viscosity	[Pa・s]
ρ	Fluid density	[kg/m^3]
	Suffices	
0	Value of entire heat exchanger	
	Superscript	
-	Average	

REFERENCES

Hesselgreaves, J. E., (2001). *Compact Heat Exchangers, Selection, Design and Operation*, pp. 1-2, Pergamon.

Kato, Y., Nitawaki, T. and Muto, Y., (2004)." Medium Temperature Carbon Dioxide Gas Turbine Reactor", *Nucl. Eng. Design*, Vol. 230, pp. 195-207.

Nikitin, K., Kato, Y. and Ngo, L., (2004). "Experimental and Numerical Study of Printed Circuit Heat Exchanger Performance in Carbon Dioxide Experimental Loop", *Proc. 6th Gustav Lorentzen Natural Working Fluids Conf.*, August 29–September 1, Glasgow, UK,.

Fluent, Inc., (2003). *Fluent 6.1 User's guide*, Fluent Inc., Lebanon, NH.

Ito, T., et al.,(1990). *PROPATH: A Program Package for Thermo-physical Properties of Fluids*, Version 10.2, Corona Publishing Co., Tokyo, Japan.

Tsuzuki, N., Kato, Y., Ishiduka, T. (2005). "High performance printed circuit heat exchanger," *Heat SET 2005, Heat Transfer in Components and Systems for Sustainable Energy Technologies*, April 5–7, Grenoble, France.

Ngo, L., Kato, T., Nikitin, K. and Tsuzuki, N.(2005),"New printed circuit heat exchanger with S-shaped fins for hot water suppliers," *Proc. ECI International Conference on Heat Transfer and Fluid Flow in Microscale*, Castelvecchio Pascoli, Italy, September 25-30